PROCEEDINGS, Thirty-Ninth Workshop on Geothermal Reservoir Engineering
Stanford University, Stanford, California, February 24-26, 2014
SGP-TR-202

The Blackfoot Volcanic Field, Southeast Idaho: A Hidden High-Temperature Geothermal Resource in the Idaho Thrust Belt

John Welhan[1], Mark Gwynn[2], Suzette Payne[3], Michael McCurry[4], Mitchell Plummer[3] and Thomas Wood[5]

[1] Idaho Geological Survey, University of Idaho, Moscow, ID 83844-3014

[2] Utah Geological Survey, Salt Lake City, UT 84114-6100

[3] Idaho National Engineering Laboratory, Idaho Falls, ID 83415

[4] Dept. of Geosciences, Idaho State University, Pocatello, ID 83209-8072

[5] University of Idaho, Center for Advanced Energy Studies, Idaho Falls, ID 83402

e-mail: John Welhan <welhjohn@isu.edu>

Keywords: Idaho-Wyoming thrust belt, hidden geothermal, magmatic hydrothermal

ABSTRACT

For more than thirty years since southeast Idaho's Blackfoot volcanic field (BVF) was listed as a "Known Geothermal Resource Area," exploration based on a conventional Basin and Range volcanic paradigm has failed to confirm the existence of a high-temperature resource. Now, a synthesis of data compiled for the National Geothermal Data System (NGDS) has identified a previously unrecognized high-temperature prospect within the Idaho thrust belt (ITB) adjacent to the BVF (Welhan et al., 2013), explaining the hidden nature of this magmatic geothermal system, and why it has remained hidden to conventional exploration for so long.

Volcanologic and geohydrologic evidence suggests that a significant amount of unerupted magma remains at a depth of 12 to 14 km beneath the BVF's 58 ka rhyolite domes at China Hat. The magnitude of the CO_2 flux in the southern BVF, rivalling that of many active quiescent volcanoes, and the presence of magmatic helium in these volatiles confirms that a robust magmatic heat source is still actively outgassing (Lewicki et al., 2012).

Thermal data from deep wildcat petroleum wells and new heat flow data compiled for the NGDS were evaluated in the context of the structural and stratigraphic architecture of the western ITB. This analysis suggests that magmatic hydrothermal fluids are channeled from depths of 10 km or more beneath the BVF, moving eastward out of the graben along regional thrust faults and permeable Paleozoic and Mesozoic strata, into reservoirs at depths of 3-5 km in the adjacent ITB. The sodium-chloride nature of high-temperature fluids encountered by wildcat wells and the coincidence of microseismic swarms in the area where Jurassic salt beds are believed to be thickest suggest that these magmatic hydrothermal fluids are actively enhancing the bulk porosity and permeability of potential reservoir rocks via dissolution of massive salt beds, leading to localized roof collapse and seismicity.

The thermal data derived from historic wildcat petroleum wells in the ITB defines a band of high heat flow, some 20 to 50 km north and southeast of China Hat, over an area of hundreds of square kilometers. Heat flows of 100 to 220 mW/m^2 coincide with the presence of hot (160-220 ^oC) sodium-chloride fluids at depths of 3-5 km in limestone and sandstone reservoir rocks of Pennsylvanian to Jurassic age. The presence of sodium-chloride thermal springs in other parts of the western thrust belt (e.g., Heise Hot springs, Maple Grove prospect, Crystal Hot Springs, Renaissance prospect) suggests that thermal reservoirs of this type exist in other parts of the Idaho-Utah thrust belt in similar structural settings.

1. INTRODUCTION

The Blackfoot Reservoir - Gray's Lake area of southeast Idaho, in which the Blackfoot Volcanic Field (BVF) is found (Figure 1), was considered "one of the most favorable geothermal prospects in Idaho, based on regional geology. Voluminous Pleistocene basaltic lava flows . . . overlain by younger rhyolite, the Intermountain Seismic Belt . . . [and] thermal springs suggests the presence of an important heat source" (IDWR, 1980; Mitchell et al., 1980). The residual thermal energy of the China Hat rhyolite's presumed magma reservoir was estimated at 7 x 10^{10} MW_t-hours, equivalent to that of the Newberry Crater resource (Smith et al., 1978; Smith and Shaw, 1979). Despite this early attention, however, interest in the BVF's geothermal potential has all but disappeared for lack of evidence of a high-temperature resource at drillable depth. McCurry and Welhan (2012) have pointed out that geochemical data indicates the BVF rhyolites, like the Quaternary rhyolite eruptive systems of the eastern Snake River Plain, are also the product of extreme differentiation of a large-volume, mid- to upper crustal magma chamber and therefore would be expected to represent a still-robust magmatic heat source. However, if a body of hot magma still exists beneath the BVF, then a paradox presents itself: Why is this heat not expressed more obviously at the surface? Other than a few warm springs (T_{max} = 40 ^oC) and large travertine deposits, there are no compelling manifestations of such a youthful magmatic heat source. The SunHub 25-1 exploratory well, drilled in 1981 to a depth of 2.36 km just south of China Hat, encountered a bottom-hole temperature of only 69 ^oC (NGDS, 2012), suggesting that the magmatic heat reservoir is already spent or that the BVF is the quintessential hidden geothermal resource. Based on published reconstructions of the Idaho thrust belt's (ITB) subsurface architecture in this region, Autenreith et al. (2011) first postulated that heat from the magma may be diverted laterally along regional thrust faults, leading to speculation that the hydrothermal resource may be located east of the graben, in sedimentary rocks of the ITB. The objective of this paper is to examine this hypothesis, refine it with available geohydrologic and geothermal data culled from the National Geothermal Data System (NGDS) data compilation effort, and identify testable hypotheses that can help bring closure to this long-standing debate.

2. GEOHYDROLOGIC SETTING

2.1 Geologic Context

The BVF is a bimodal complex of Quaternary-age basalt lava flows and rhyolite domes in the northeastern-most part of the Basin and Range (B&R) province where the B&R transitions into the ITB (Figure 1). The volcanic field occupies two major grabens as well as numerous topographic valley lows, extending in a roughly north-south orientation from about 20 km south of the eastern Snake River Plain's (ESRP) southern margin to about 90 km south. The crustal framework is dominated by thick (ca. 40 km) Archean to early Proterozoic crust overlain by 6-10 km of late Proterozoic to Mesozoic carbonate, clastic and evaporite deposits.. These rocks were stacked eastward in extensive thrust sheets during Laramide, Sevier and older orogenies (Armstrong and Oriel, 1965; Harbour and Breckenridge, 1980; Ralston et al., 1983). The Meade thrust has been dated as Early Cretaceous to Eocene age. Rocks of the Meade thrust plate are of Mississippian to Recent age with rocks prior to the Cretaceous having a total conformable thickness of approximately 7300 m. Prior to the Cretaceous, lithologies are predominately limestone, dolomite, shale and quartz sandstone. Up to several hundred meters of Miocene to Pliocene silicic tuffs, tuffaceous sediment and lacustrine deposits of the Salt Lake Formation underlie the basalt lavas (Armstrong, 1969). Basin and Range normal faulting began in the mid-Miocene in response to east-west extension and interaction with the Yellowstone-ESRP hot spot track. The latest ESRP magmatic phase began during the late Pliocene and continued through the Quaternary, concurrent with bimodal olivine tholeiite - rhyolite volcanism in the Willow Creek-China Hat and Gem Valley grabens (McCurry and Welhan, 2012).

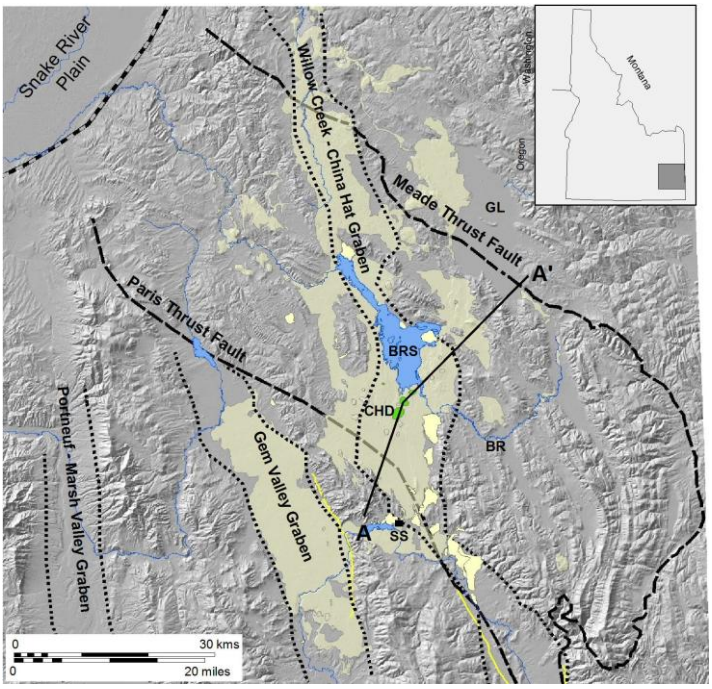

Figure 1 - Location of the Blackfoot volcanic field (shaded light yellow) relative to the eastern Snake River Plain and southeast highlands of the Idaho thrust belt. The 58 ka rhyolite domes are shown in green and travertine deposits are in white; major active Quaternary faults are shown in yellow. Dotted lines indicate Basin and Range grabens. The Paris and Meade thrust faults (heavy dashed lines) define the approximate western extent of the Idaho thrust belt to the east. Cross-section A-A' refers to Figure 2. Abbreviations used: (BRS) Blackfoot Reservoir; (BR) Blackfoot River; (GL) Gray's Lake; (SS) Soda Springs; (CHD) China Hat domes.

Basalts and rhyolites of the BVF have chemical and mineralogical affinities that are similar to those of the ESRP (Pickett, 2004; Ford, 2005; McCurry and Welhan, 2012). Volcanological features of the volcanic rocks are also similar to the ESRP, but appear to be more strongly influenced by local extensional tectonics (Pickett, 2004; McCurry and Welhan, 2012). Some 50 km^3 of olivine tholeiite basalts compositionally like the ESRP were extruded over an area of 1350 km^2 in the Gem Valley and Willow Creek-China Hat grabens, averaging 35-50 m thick and up to 220 m in the central China Hat graben (Welhan, 2014). During the latest volcanic episode starting between 58 and 70 ka (Heumann, 1999; Schmitt, 2011), the three rhyolite lava domes at China Hat were emplaced just south of what is now the Blackfoot Reservoir (Figure 1). Essentially coeval with this event, several tens of cubic kilometers of basaltic and/or rhyolitic dikes intruded the upper crust in the China Hat graben, creating a well-defined volcanic rift zone that extends over 20 km north and south of the rhyolite domes (Polun et al., 2010; Polun, 2011).

The source responsible for this latest eruptive phase is believed to be a silicic magma chamber located beneath the China Hat rhyolite domes at a depth of 12-14 km, as constrained by hornblende thermobarometry (Ford, 2005). Figure 2 shows a conceptual model by Autenreith et al. (2011) based on Dixon's (1982) structural reconstructions of the ITB, showing the position of the magma reservoir. The magma is thought to be located beneath the China Hat rhyolite domes at a depth of 13 km. Ford's (2005) thermobarometry indicates that the magma pooled near the boundary between denser Archean crystalline rocks and less dense late Precambrian sedimentary rocks and very near the intersections of the Meade and Absaroka thrust faults.

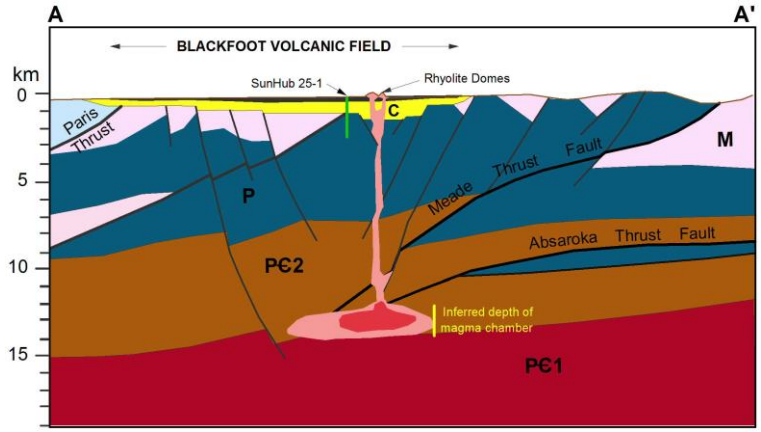

Figure 2 - Cross section A-A' of Figure 1, after Autenrieth et al. (2011), showing a conceptual model of the Blackfoot volcanic field's structural and stratigraphic context within the China Hat graben and western Idaho thrust belt, based on structural reconstructions of the ITB by Dixon (1982). The magma chamber is assumed to lie directly beneath the rhyolite domes, where thermobarometry places it at or very close to the crustal density contrast between Precambrian basement (PC1) and metasedimentary rocks (PC2). Paleozoic rocks (P) are shown in blue and Mesozoic rocks (M) in pink; Cenozoic sediments and volcanics (C) and Quaternary basalts within the China Hat graben are shown in yellow and black, respectively. SunHub 25-1 is a 2.4 km-deep geothermal exploration well.

2.2 Hydrologic and Hydrochemical Context

The study area is characterized by low to moderate precipitation. Valley precipitation at eight weather stations is typically 35-50 cm annually (WRCC, 2013), with snow water equivalent of mountain snowpack ranging from 40 to 70 cm per year, depending on elevation. Mean annual air temperatures range from 3.4 to 6.1 ^{o}C, with a lapse rate of 6.4 ^{o}C/km.

Thrust faults, normal faults and tear faults likely play an important role in controlling the movement of thermal and non-thermal fluids in the ITB (Ralston et al., 1983). Robust local- and regional-scale ground water flow systems characterize the study area (Dion, 1974; Ralston et al., 1983), supported by the availability of local recharge, topographic relief of 200-1000 m and abundant fracture porosity. The sedimentary formations responsible for hosting the most significant ground water flow are those with the greatest fracture porosity: the Pennsylvanian Wells formation (fractured limestone), the Triassic Thaynes and Dinwoody Formations (limestone and fractured limestone / siltstone, respectively), the Jurassic Stump and Nugget Sandstones and the Jurassic Twin Creek Limestone (Ralston and Williams, 1979; Ott, 1979; Ott, 1980; Simplot, 2005, 2010; USFS, 2011). The Wells Formation, in particular, is thought to be of regional significance as a water-bearing formation (Buck and Winegar, 2003).

Figure 3 summarizes published major ion data on thermal and non-thermal springs in the study area (Mitchell, 1976; Hutsinpiller and Parry, 1985; Avery, 1987), including unpublished data from Idaho State University (N. Semenza, written comm., 2012). In general, major anion ratios are non-specific except for waters of the Sulfur Canyon area. Major cations are more discriminating, but the greatest specificity is seen in the cross-plot field where two trends segregate spring chemistries according to geographic position in the BVF. In the southern BVF (inset, Figure 3), waters are Ca-Mg-HCO_3 in composition with neutral to slightly alkaline pH; waters in the northern BVF are similar but have a clear Na-Cl component (not as evident in the anion field but clearly expressed in bivariate plots). In contrast, the acid-sulfate waters of the Sulfur Canyon area southeast of Soda Springs have a vapor-dominated character (White et al., 1971), consistent with their low pH (2.8-4.8) and vigorously effervescing pools and soils. Several springs define a possible fourth group in the cation field that is not geographically specific, possibly indicating that the Na-Cl component manifests to varying degrees depending on local fluid pathways and water-rock interactions.

2.3 Geothermal Context

Recent work on the flux of CO_2 in the southern BVF has provided compelling evidence of the impact of volcanic outgassing in this part of the graben (Lewicki et al. 2012) and corroborates the existence of a robust magmatic heat source beneath the BVF. Based on a ^{13}C mass-balance, Lewicki et al. argue that more than half of the CO_2 flux in the southern BVF is of deep origin; its elevated $^{3}He/^{4}He$ ratios (1.8 - 2.4 R_a) confirm that a significant fraction of the volatile flux is magmatic in origin. Based on CO_2 discharge in springs and atmospheric eddy-flux measurements, Lewicki et al. determined that CO_2 flux in the southern BVF was as much as 350 tons/day, comparable to CO_2 emission rates observed over quiescent active volcanoes. Their data also indicate that the Sulfur Canyon area has an unusually high CO_2 flux, possibly with a sulfurous component, that is consistent with hydrogeochemical indications of its vapor-dominated nature.

However, no evidence of high-temperature discharge, either past or present, exists anywhere in the BVF. All features plotted in Figure 3 have water discharge temperatures no greater than 40 ^{o}C, most are less than 30 ^{o}C, and geothermometry estimates based on those data are no higher than 100 to 110 ^{o}C (Mitchell, 1976; Reed and Spycher, 1984; Hutsinpiller and Parry, 1985). If a high-temperature fluid does make its way to the surface in this graben, it must re-equilibrate at lower temperatures within shallow aquifers and/or be drastically diluted by shallow ground water. The SunHub 25-1 exploratory well, just south of China Hat, was drilled in 1981 to a depth of 2.4 km. While the maximum temperature reported during drilling was 98 ^{o}C between 2.0 and 2.25 km, the bottom-hole temperature when logged was just 69 ^{o}C (NGDS, 2012). Assuming that the magmatic heat source is as robust as Lewicki et al.'s (2012) data suggest, then, this geohydrologic system must be the quintessential hidden geothermal resource.

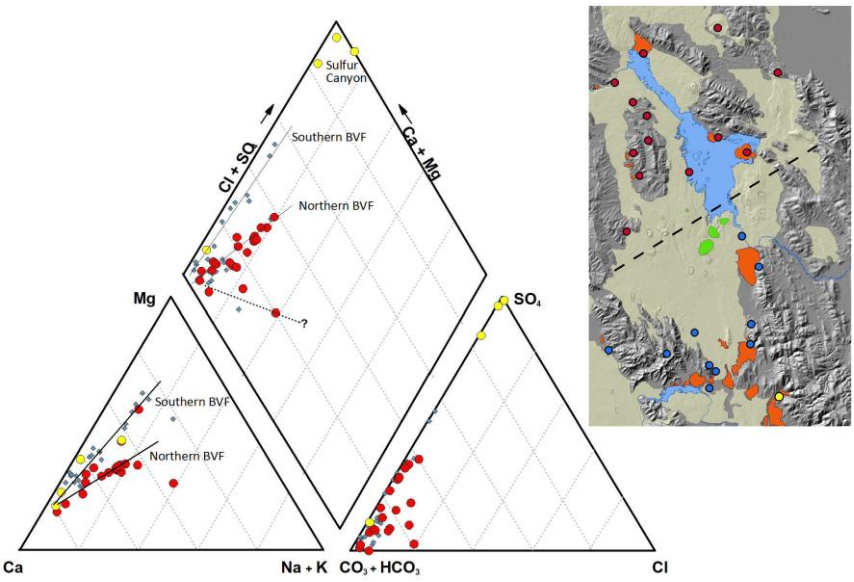

Figure 3 - Piper plot of available major ion data for thermal and non-thermal springs in the Blackfoot volcanic field (beige on inset map). Different water compositions northwest and southeast of China Hat are shown as red and blue symbols, respectively; springs in the Sulfur Canyon area are shown in yellow. Travertine terraces are shown as orange and rhyolite domes, as green. Dashed line in the inset shows approximate geographical division between northern and southern compositional differences in the Piper plot.

2.3.1 Shallow Heat Flow Data

The study area's background heat flow reflects the response of the continental lithosphere to passage of the Yellowstone hotspot as well as to crustal extension and upwelling of mantle heat that characterize the B&R as a whole (Blackwell, 1989). In what follows, the area of the B&R province south of the ESRP will be referred to as the Great Basin.

Few reliable heat flow estimates are available for southeast Idaho. As on the ESRP, shallow heat flow measurements in the BVF tend to be low because of advective overprinting by ground water flowing in the shallow basalt aquifer (Brott et al., 1976). Similar effects are expected in the area's fractured sedimentary rocks. Of 38 wells in Southern Methodist University's heat flow database that are located in and around the BVF, fourteen are classified as having reliable information but only seven have associated heat flow estimates (SMU, 2008). Figure 4 summarizes the SMU data, showing that several shallow wells with bottomhole temperatures of less than 16 ^{o}C have heat flows ranging from 28 to 51 mW/m^2. Four locations have heat flow exceeding 120 mW/m^2, including a 2900-meter wildcat petroleum well east of the BVF whose heat flow is 126 to 184 mW/m^2 depending on the effective thermal conductivity assumed to characterize its 3020-meter length. Two other locales are noteworthy for their surprisingly high heat flow: a value of 121 mW/m^2 on the west side of Reservoir Mountain (Figure 4) and values of 138 and 167 mW/m^2 in the area of high magmatic volatile flux (Lewicki et al., 2012). In contrast, SunHub 25-1, the 2400-meter geothermal exploration well drilled 1.4 km southwest of China Hat directly over the BVF's presumed heat source, revealed a disappointingly low heat flow of 55 mW/m^2 (SMU, 2008).

As part of the NGDS project, the Idaho Geological Survey (IGS) installed three thermal gradient wells in the BVF (Figure 4) to evaluate some puzzling heat flows documented in SMU's database. Drilling and thermal gradient results for the IGS wells are detailed in Welhan (2014) and will be published to the NGDS data catalog shortly. Well B2 was drilled to 137 m near the East Gem Valley fault to evaluate heat flow in the southern Gem Valley; basalts in this area may have erupted as recently as 15 ka and several thermal springs and warm water wells are known on the west side of the valley. A respectable thermal gradient was found in the upper 30 meters of this well but the apparent heat flow (82 mW/m^2) is elevated due to upwelling of warm water along this late Quaternary fault. Well B4, north of Reservoir Mountain, was drilled to a depth of 86 meters to confirm SMU's reported heat flow for a well of unknown depth on the west side of Reservoir Mountain. Although well B4's thermal gradient defined a conductive regime, its low heat flow (50 mW/m^2) suggests that the high heat flow reported in the SMU database west of Reservoir Mountain is not representative of the area. The presence of several small travertine terraces and a shallow thermal anomaly in that area (Mitchell, 1976) suggests that, as in the case of well B2, the high heat flow value in SMU's database also reflects upwelling of warm water; therefore, this value is discounted in subsequent evaluations of heat flow patterns. Well B3 was drilled to 107 m near the Meade thrust fault and revealed a purely conductive thermal gradient and heat flow of 93 mW/m^2, confirming that elevated heat flow occurs northeast of the BVF and that the Gentile Valley 9-1 well, SMU's highest heat flow value, is not an isolated anomaly.

Compared to data on the Great Basin, heat flow values observed in the BVF are not unusual. Blackwell (1983) estimated that the Great Basin's average heat flow is of the order of 100 ± 10 mW/m^2, significantly higher than the mean crustal heat flow of 65 mW/m^2 (Pollack et al., 1993). Lachenbruch and others (1994) reported mean heat flow values in the northern Great Basin of 92 ±9 mW/m^2 and 82 ± 3 mW/m^2 in the southern Great Basin. Henrikson and Chapman (2002) reported a mean heat flow in Utah's B&R province of 91 mW/m^2 based on 181 wells, although this value reflects several wells in the Great Salt Lake basin that average 115 mW/m^2.

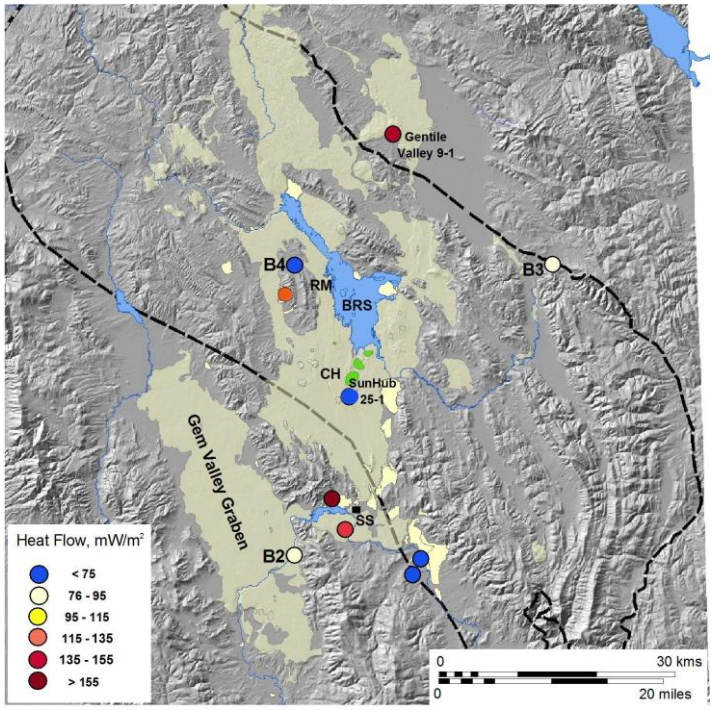

Figure 4 – Available heat flow data within the study area, from SMU's (2008) database and from recent shallow thermal gradient wells (B2, B3, B4) that were installed with NGDS funding. Abbreviations used: (RM) Reservoir Mountain; (GV) Gem Valley; (BRS) Blackfoot Reservoir; (CH) China Hat; (SS) Soda Springs.

3. THRUST BELT DATA

Beyond information available from shallow wells and springs, historic petroleum well drilling in the ITB has provided considerable information that has not heretofore been recognized or synthesized in a geothermal context. In what follows, data on deep petroleum well temperatures, heat flow, lithology and fluid chemistry collected for the NGDS (2012) are presented, together with a preliminary examination of historic seismic data collected by the Idaho National Laboratory in this part of the Idaho thrust belt.

3.1 Deep Wells in the Idaho Thrust Belt

3.1.1 Stratigraphic and Structural Context

Figure 5 shows the locations of deep petroleum wells in the ITB for which thermal data are available, as well as the stratigraphic and structural context of selected wells that encountered high-temperature fluids during drilling. The numbered cross sections correspond to Dixon's (1982) reconstructions of thrust belt architecture in the region. Also shown are key stratigraphic units that are known to host productive fluid reservoirs in the thrust belt: the Twin Creek Formation (Jurassic), Nugget Sandstone (Jurassic), Dinwoody Formation (Triassic) and the Wells Formation (Pennsylvanian). The Jurassic Preuss Sandstone is also shown because it contains massive salt beds that may play a key role in this system (Section 3.2).

3.1.2 Heat Flow Estimates

Table 1 summarizes available bottom–hole temperature (BHT) data in petroleum wells for which geophysical logs with temperature data and drill stem test (DST)–derived temperatures are available (NGDS, 2012). These wells range in depth from 0.9 to 5 km, with uncorrected BHTs of 49 to 222 ^{o}C. Not all deep wells in the region encountered high temperatures, however. Maximum uncorrected temperatures in three of the northeastern-most and four of the deepest wells in the southeastern-most corner of the study area range from 81 to 122 ^{o}C at depths between 2.8 and 4.2 km.

Corrections were applied to the BHT data to offset the temperature disequilibrium effects resulting from the circulation of drilling fluids. Data were sufficient in about 75% of the wells to perform a Horner Correction for the BHT at the final TD (total depth). There were additional BHT data at intermediate depths in the majority of these wells that were corrected using Horner and/or the single BHT–time pair methods of Henrikson (2000) and Henrikson and Chapman (2002). Edwards (2013) compared the results of a suite of high–quality Horner Corrections with the single BHT–time pair methods of Henrikson (2000) and Henrikson and Chapman (2002). He assumed the Horner Corrections represent the undisturbed borehole temperature and found that the single–point corrections usually overcorrected by about 1°C with a standard deviation of 11°C. Edwards (2013) also compared the widely–used technique of Harrison et al. (1983) and a variation of the Harrison technique from Blackwell and Richards (2004). These results showed that for Utah wells the Harrison Correction tends to overcorrect by about 4°C and the SMU Correction generally under-corrects by 2°C, both with a slightly improved standard deviation of 10°C. We believe the Henrikson (2000) and Henrikson and Chapman (2002) methods also reasonably apply to these Idaho wells. Indeed, they generally correlate well with the gradients established using the more rigorous Horner–Corrected BHTs in many of the wells. The single–point method was used to

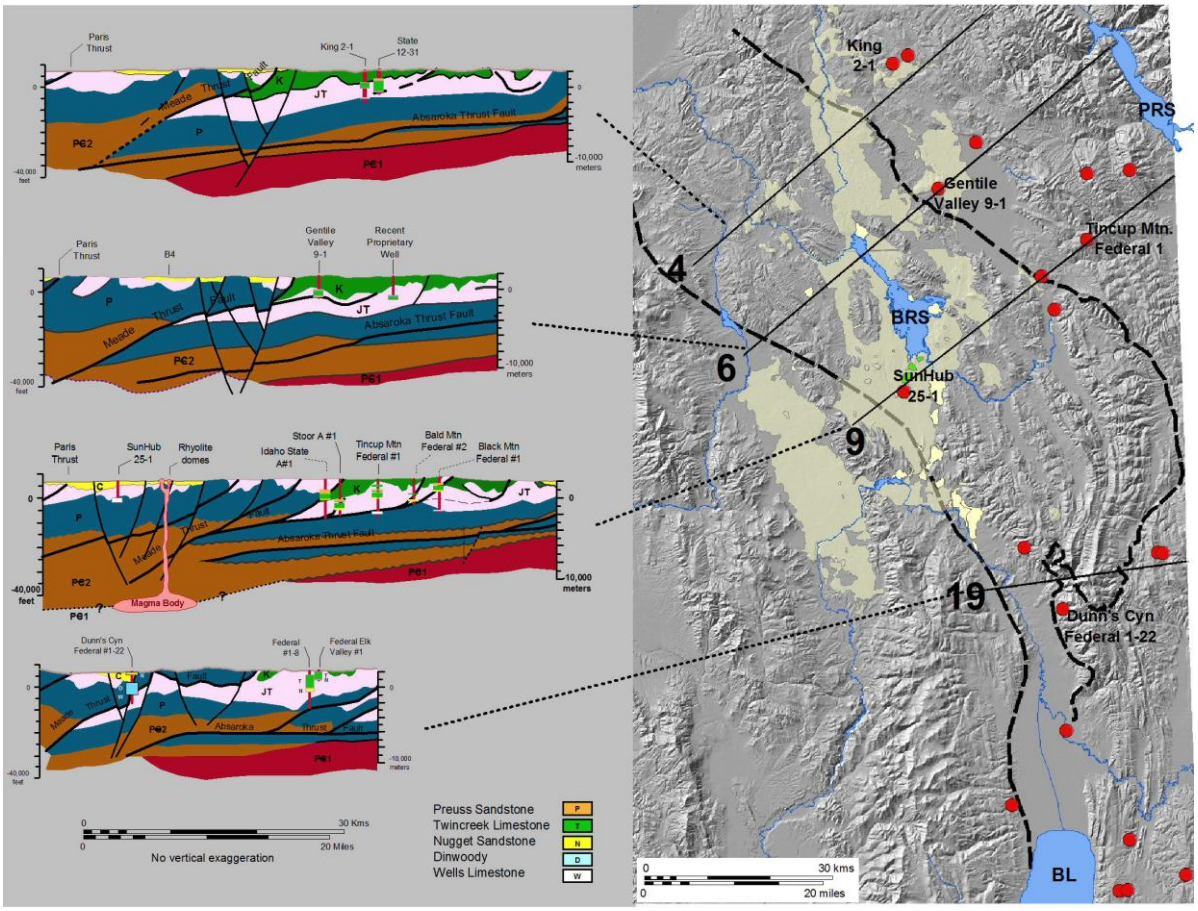

Figure 5 – Deep wells in the Idaho thrust from which heat flow estimates were derived belt (red dots on map). Selected cross sections are after Dixon (1982), showing well locations in cross sections 4, 6, 9 and 19. Also shown are several key stratigraphic units that may host productive fluid reservoirs and their positions in the cross sections. Abbreviations used: (BRS) Blackfoot Reservoir; (BL) Bear Lake; (PRS) Palisades Reservoir.

correct the final (deepest) BHT in two of the wells. In one of these, a number of intermediate, Horner–Corrected BHTs and DSTs supported the single–point correction, which consequently lends confidence to the correction in the other well. Data were insufficient to apply these methods in three wells, so the depth-dependent correction from Morgan and Scott (2011) was used.

Corrected BHT values were then converted to depth-averaged thermal gradient estimates according to:

$$(T_{BHT} - T_o)/(Z_{BHT} - Z_o),$$

where T_{BHT} is the corrected temperature at depth Z_{BHT}, and T_o is local mean annual air temperature determined from a relationship derived from data at seven local meteorological stations:

$$T_o = T_{air} + 3.0 = -6.44 * \text{altitude} + 19.73 \quad (r^2 = 0.94)$$

Altitude is in kilometers, and the +3 ^oC offset represents the difference between local mean annual air temperature and the surface-temperature intercepts observed in thermal gradient wells B2, B3 and B4. Thermal gradients were subsequently converted to heat flow by averaging the minimum and maximum heat flow estimates derived from the range of depth-averaged thermal conductivities that SMU applied in estimating Gentile Valley 9-1's heat flow (SMU, 2008). For comparison, heat flows estimated in this manner are approximately 9% higher than reported in SMU's database for Gentile Valley 9-1 and SunHub 25-1.

Figure 6 summarizes the spatial distribution of heat flow in the study area. In the vicinity of the Utah border around Bear Lake, heat flow averages 61 mW/m^2 and represents the best estimate of background heat flow in this portion of the ITB. Heat flow within the China Hat graben all the way to Bear Lake, is at background levels, averaging 57 mW/m^2. Fourteen wells immediately east of the Willow Creek-China Hat graben have heat flows greater than 75 mW/m^2, averaging 104 mW/m^2. It remains to be seen whether this area of elevated heat flow represents a continuous zone or localized, discrete areas of high heat flow. One well to the northeast of this zone suggests that heat flow may decrease in that direction, but more data are needed. The highest heat flows occur in three wells 35-50 km north of China Hat in which dense, sodium-chloride waters were encountered at depths of 3-4 km. This is also the area in which thermal and non-thermal ground water reflects a Na-Cl component (see Figure 3).

Table 1 - Heat flow estimates based on corrected thermal gradients for wildcat wells in southeast Idaho. See text for correction procedure.

Well Name	Latitude	Longitude	Surface Elevation meters	T_o °C	BHT Depth meters	Corrected BHT °C	Corrected Gradient °C/km	Estimated Heat Flow mW/m²
Wells E and NE of the BVF								
King No. 2-1	43.2796	-111.6150	2012	6.8	4140	211	49.3	121
Black Mtn Federal No.1	43.1087	-111.1347	2495	3.7	4159	121	28.2	69
Gentile Valley 9-1	43.0900	-111.5300	2080	6.3	3008	186	61.2	150
Bald Mountain No. 2	43.1055	-111.2225	2370	4.5	2749	104	36.2	89
Tincup Mtn. Federal No.1	43.0065	-111.2273	2456	3.9	5056	191	37.0	91
Idaho State "A" No. 1	42.9030	-111.2983	2038	6.6	4979	185	35.8	88
Proprietary well	43.1577	-111.4487	1954	7.1	2865	232	78.5	192
Stoor "A" #1	42.9535	-111.3223	2059	6.5	4510	192	41.1	101
State No. 12-31	43.2911	-111.5839	2057	6.5	2965	116	36.9	90
Wells in the BVF								
SunHub 25-1	42.7867	-111.6117	1890	7.6	2388	78	30.0	72
Wells S and SE of the BVF								
Big Canyon Federal No. 1-13	42.5471	-111.3750	2067	6.4	3558	173	46.8	115
Federal No. 1-8	42.5337	-111.1033	2343	4.6	4916	158	31.2	76
Federal Elk Valley No.1	42.5324	-111.0944	2284	5.0	1193	48	36.0	88
Dunn's Canyon Federal No.1-22	42.4528	-111.3021	2133	6.0	4079	148	34.8	85
Jensen No. 22-1	42.2710	-111.3013	1812	8.1	3499	97	25.4	62
North Eden Federal No.21-11	42.0268	-111.2042	2114	6.1	2865	86	27.9	68
N. Rabbit Ck. Federal No. 6-21	42.0277	-111.1887	2055	6.5	3538	81	21.1	52
Grace Federal No. 10-1	42.0478	-111.0683	2325	4.8	3616	84	21.9	83
Worm Creek No.1	42.1615	-111.4169	1846	7.8	2284	53	19.8	48
Federal DI No.1	42.1033	-111.1802	1940	7.2	3056	76	22.5	55

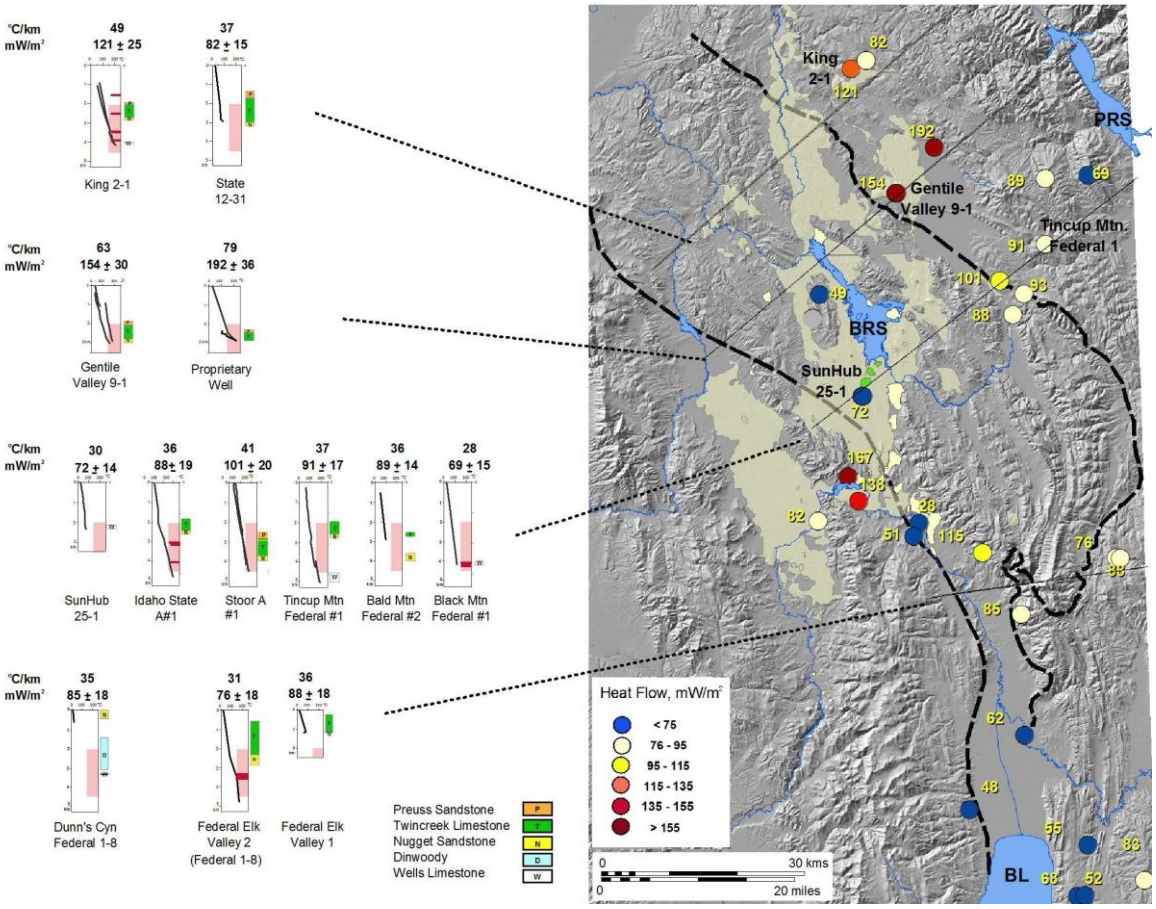

Figure 6 – Summary of all heat flow data in the study area, together with information on selected deep wells along Dixon's (1982) cross sections 4, 6, 9 and 19, indicated on the map. All thermal gradient plot scales are 0-200 °C; pink shaded zones indicate the economic target zone defined by Allis et al. (2013) for developing hot sedimentary reservoirs (T >160 °C at depths from 2 to 4.5 km). Red bars shown on some temperature logs indicate where fluid chemistry data are available (Table 2). Corrected thermal gradients are indicated above each plot, and heat flows are shown in yellow text on the map as well as over each thermal gradient plot. Abbreviations used: (BRV) Blackfoot Reservoir; (BL) Bear Lake; (PRS) Palisades Reservoir.

3.2 Composition of High-Temperature Fluids

Table 2 lists all available fluid chemistry data compiled from DSTs in six wildcat wells drilled in the study area as well as data for a thermal spring (Heise) and well (East Bingham) outside of the immediate study area that have similar, possibly related, compositions. Figure 7 shows a Piper plot of the major-ion data in Table 2. Analytical or accuracy information is not available in the DST reports, but charge balance errors average 2% and indicate a reasonable level of analytical accuracy overall. Total dissolved solids in the deep wells averages 60,000 mg/liter, but values range as high as 320,000 mg/liter. The solubility of NaCl in water at 100 ^{o}C and atmospheric pressure is approximately 390,000 mg/liter (Clarke and Glew, 1985), so the densest brine samples approach halite saturation. The average pH is 8.5, with a third of the samples having pH between 9 and 11.1.

Table 2 – Chemical composition data for thermal fluids encountered in deep wells drilled in the ITB, summarized from drill stem test reports (NGDS, 2012). Also shown are data for a shallow thermal well and thermal springs in the region.

Sample Site	Source	Depth, meters	T, °C	pH	Ca	Mg	Na	K	Cl	SO_4	HCO_3	TDS	Li	Ba	Fe	SiO_2	F	B
Idaho State A No.1	DST	4016 - 4036	n.a.	9.0	55	2	125537	177	190000	4600	683	320809						
	DST	4016 - 4036	n.a.	8.4	233	5	121400	185	185000	3600	329	310597						
	DST	4016 - 4036	148	9.4	94	1	2716	17	290	3710	1927	7968						
	DST	4016 - 4036	148	9.4	49	0	1133	6	120	1274	1049	3241						
	DST	4016 - 4036	148	11.1	90	0	11781	22	1650	2934	5862	25950						
	DST	3082 - 3084	126*	8.8	5	0	7232	65	9200	2790	235	19549	113					
	DST	3082 - 3084	126*	6.9	1051	173	32965	561	38400	2140	2415	68478						
	DST	3082 - 3084	126*	7.0	769	151	23854	440	36200	2330	1854	64656						
	DST	3082 - 3084	126*	6.2	673	178	25894	572	39900	2080	1267	69920						
King No.2-1	H. Neupane, 2013	326	160	-	1598	1498	46946	2098	76912	5594	135	11600						
	H. Neupane, 2013	3809	160	6.6	71	27	163	39	282	66	224	20567						
	Ralston et al, 1983	2606 - 2639	116	7.4	430	46	9400	470	6900	9400	3300	28000						
	Ralston et al, 1983	3467 - 3511	160	6.6	170	43	19000	2100	27000	1800	4000	52000						
	Ralston et al, 1983	3910 - 3927	249	8.0	210	0	18000	2600	26000	1800	4500	50000						
Black Mtn Federal No.1	DST	4131 - 4176	116	8.4	252	28	5777	138	4800	3189	4026	16227						
	DST	4131 - 4176	116	8.4	183	39	5009	95	3700	3197	3660	14079						
	DST	4131 - 4176	116	8.8	183	14	6070	166	5700	2828	3258	16733						
	DST	4131 - 4176	n.a.	7.4	430	17	8177	500	10200	2564	3074	23402						
	DST	4131 - 4176	n.a.	8.5	89	20	2833	32	950	3025	2294	8163						
	DST	4131 - 4176	n.a.	8.1	243	28	6396	185	6400	2967	3367	17877						
	DST	4131 - 4176	n.a.	6.9	131	6	8584	485	10500	2823	2318	23671						
	DST	4130 - 4176	65	6.9	130	6	8600	490	11000	2800	2300	24000						
Elk Valley #2 Federal No. 1-8	DST	3470 - 3501	149	10.2	142	36	4000	-	3965	1350	1749.4	11600		3.8	148			
	DST	3549 - 3622	114	9.7	203	15	7239	87	2000	7600	5856	20567						
North Eden Federal 22-11	Ralston et al, 1983	2504 - 2581	92	9.8	39	2	6500	130	600.0	11000	3100.0	19000						
Jensen 22-1	DST	3322 - 3332	74	10.5	30	0	8400	93	1100.0	11000	7000.0	29000						
E. Bingham Well	Ralston et al, 1983	-	63	6.2	320	36	4600	770	7800.0	48	930.0	27999						
Heise Hot Springs	USGS, 2012	-	48	6.7	430	85	1530	192	2360	756	1080	5950	2.3		0.1	33	3.1	4.6

* as measured in DST #3, 3084-3115 interval

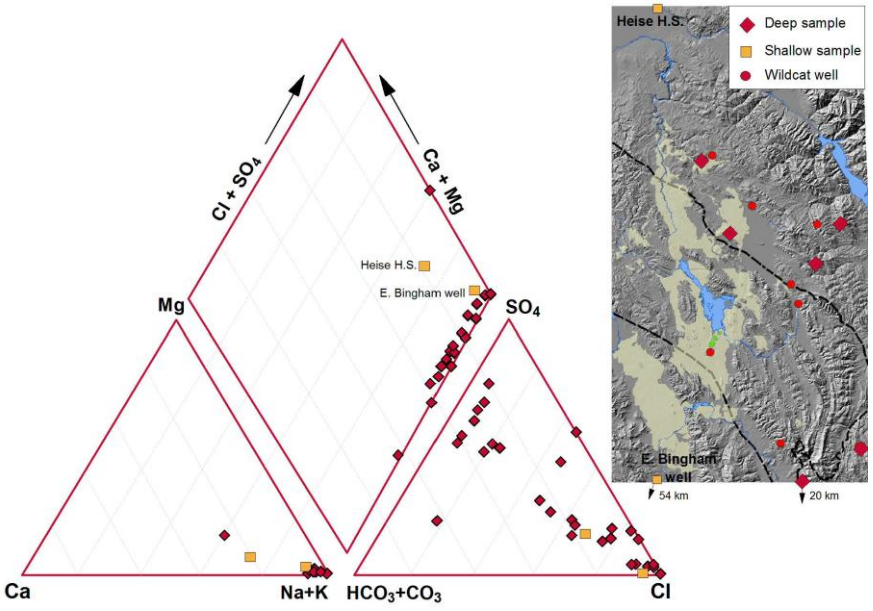

Figure 7 – Major ion compositional trends of samples shown in Table 2. The inset map indicates locations of samples that are plotted in the Piper diagram and also where brine was encountered but data are not available. The locations of Heise Hot Spring, a saline fluid of similar composition to the deep brines and the East Bingham thermal well are shown on the inset map. Data are from Welhan (2014) and Ralston et al. (1983).

The source of the dissolved salt appears to be the Jurassic Preuss Sandstone which contains massive halite beds up to several hundred meters cumulative thickness (NGDS, 2012; IGS, 2013), as well as minor amounts of gypsum and anhydrite that occur throughout the stratigraphic section. The chemistry of these formation fluids suggests that halite plus variable amounts of anhydrite and/or gypsum are being dissolved by hydrothermal fluids migrating out of the China Hat graben into Mesozoic rocks of the ITB. Dissolution of considerable amounts of halite could significantly enhance secondary porosity, even leading to localized destabilization and roof collapse if enough "solution mining" occurs. If this is the case, then shallow seismicity might be observable in the area.

The lithium concentration of these brines may be noteworthy. In the sole sample for which an analysis is available (Table 2), lithium concentration is 113 mg/liter, approaching the lower limit seen in Salton Sea geothermal brines where a demonstration plant has been extracting essentially pure $LiCO_3$ from the hot brines feeding a geothermal power plant (EERE, 2011; Mulvaney and Kaskey, 2012). The chloride content of the sample in question, however, has been diluted by 95% relative to the maximum concentration observed in the adjacent DST interval (Table 2). At this Li/Cl ratio (1280 times seawater), the lithium concentration would exceed 2000 mg/liter in the undiluted brine, five times higher than the Salton Sea brines. Hofstra et al. (2013) have pointed out that lithium-rich rhyolite melt inclusions (and, by extension, magmatic-hydrothermal outgassing) may be the source of very high lithium concentrations in sedimentary basin brines associated with topaz rhyolites. For comparison, whole-rock lithium contents in China Hat (a topaz rhyolite) range up to 105 ppm which is at the high end of whole-rock analyses reported by Hofstra et al. (2013) for rhyolites such as Spor Mountain, western Utah. In contrast, melt inclusions in Spor Mountain volcanics contain up to 5000 ppm lithium. Hofstra et al. speculate that volcanic eruptions could release "enormous amounts of lithium" into nearby sedimentary basins.

3.3 Historical Microseismicity

Figure 8 summarizes earthquakes for the period 1981 through 2012 in the study area, together with heat flow and subsurface information relevant to the possible genesis of seismicity. The earthquakes were located by the Idaho National Laboratory's (INL) seismic monitoring program, which includes analysis of INL's seismic stations and nearby stations from other agencies. Over the 30 year period, seismic station density has increased in the study area and includes EarthScope's Transportable Array stations operating from 2007-2009 (USArray, 2013). The seismicity in Figure 8 is characterized by a number of earthquake swarms that have occurred at different time periods and locations. Swarm activity in southeast Idaho was recognized by Bones (1978). The only non- swarm activity was the 1994 Draney Peak sequence near Afton, Wyoming which included a magnitude 5.8 mainshock and several magnitude 5+ earthquakes in its aftershock sequence.

This seismicity, with its distribution of epicenters and predominance of swarm activity, may prove critical for deciphering the nature of the geothermal system in this part of the ITB, if accurate information on focal mechanisms and depths can be extracted. The concentration of seismicity coincides with the area of high heat flow, the occurrence of saline fluid, and the presence of massive halite beds in the subsurface. Because the earthquake swarms could indicate locations of fluid movement or activity on faults related to magmatic or dissolution processes, such as has been observed due to roof collapse during solution mining of salt (Whyatt and Varley, 2013), further analysis is planned.

4. CONCEPTUAL MODEL AND HYPOTHESES

Figure 9 depicts a two-dimensional conceptual model of geohydrologic architecture in the vicinity of the China Hat graben and some of the hydrodynamic and thermal boundary conditions that need to be explored to explain the distribution of heat in the ITB. The interplay between regional-scale ground water flow and the possible effects of thermally driven buoyant flow as well as the effect of density-driven flow on mass and heat transport are indicated. A number of questions and hypotheses need to be examined but have not yet been evaluated quantitatively.

4.1 Summary of Relevant Observations

High Heat Flow Outside the China Hat Graben – No conclusive evidence exists for a high-temperature resource at depth within the China Hat graben. Rather, the resource is located in the ITB east of the graben's 58 ka rhyolite domes whose magmatic source is thought to sustain the hydrothermal system. Heat flow in deep petroleum wildcat wells 10-30 km east of the China Hat graben ranges from 100 to 200 mW/m^2 and defines an elongated band of elevated heat flow in the ITB.

Stratigraphic and Structural Context – This heat flow anomaly is situated immediately east of the China Hat graben where the western thrust belt is cut by normal faults of the northeastern-most part of the Great Basin. Geothermal fluids have been encountered in middle Mesozoic to late Paleozoic rocks of the Meade and lower Absaroka thrust plates and are associated with rocks of the Jurassic Preuss Sandstone, Twin Creek Limestone, and Nugget Sandstone, the Triassic Dinwoody Formation and the Pennsylvanian-Permian Wells Formation (both limestones), all of which are known to be productive hydrocarbon reservoirs in the Wyoming and Utah portions of the thrust belt and, in the study area, prolific ground water producers at shallow depths.

Geothermal Reservoir Potential – Thermal logs from deep wells in the ITB show that corrected temperatures of 160-230 ^oC occur at depths of 3-5 km within the economic target range defined by drilling and production considerations in hot sedimentary basins (Allis et al., 2013). Hot fluids have been encountered in, and sampled from, several formations that have reservoir potential. Given the large areal extent of the heat flow anomaly east of the BVF, the total volume of producible fluid may be quite large.

Chemical Composition of High-Temperature Fluids – The hot fluids encountered in the ITB are thought to be the result of advective heat transport from a magmatic hydrothermal source, ascending along structurally and/or stratigraphically controlled flow paths from 10-12 km beneath the China Hat graben into shallower sedimentary reservoirs of the ITB. The fluids have a distinct Na-Cl ± SO_4 composition with salinities that range up to levels similar to Salton Sea geothermal brines; they are likely the product of dissolution of massive halite interbeds within the Preuss Sandstone as well as minor anhydrite and gypsum that occur throughout the stratigraphic section.

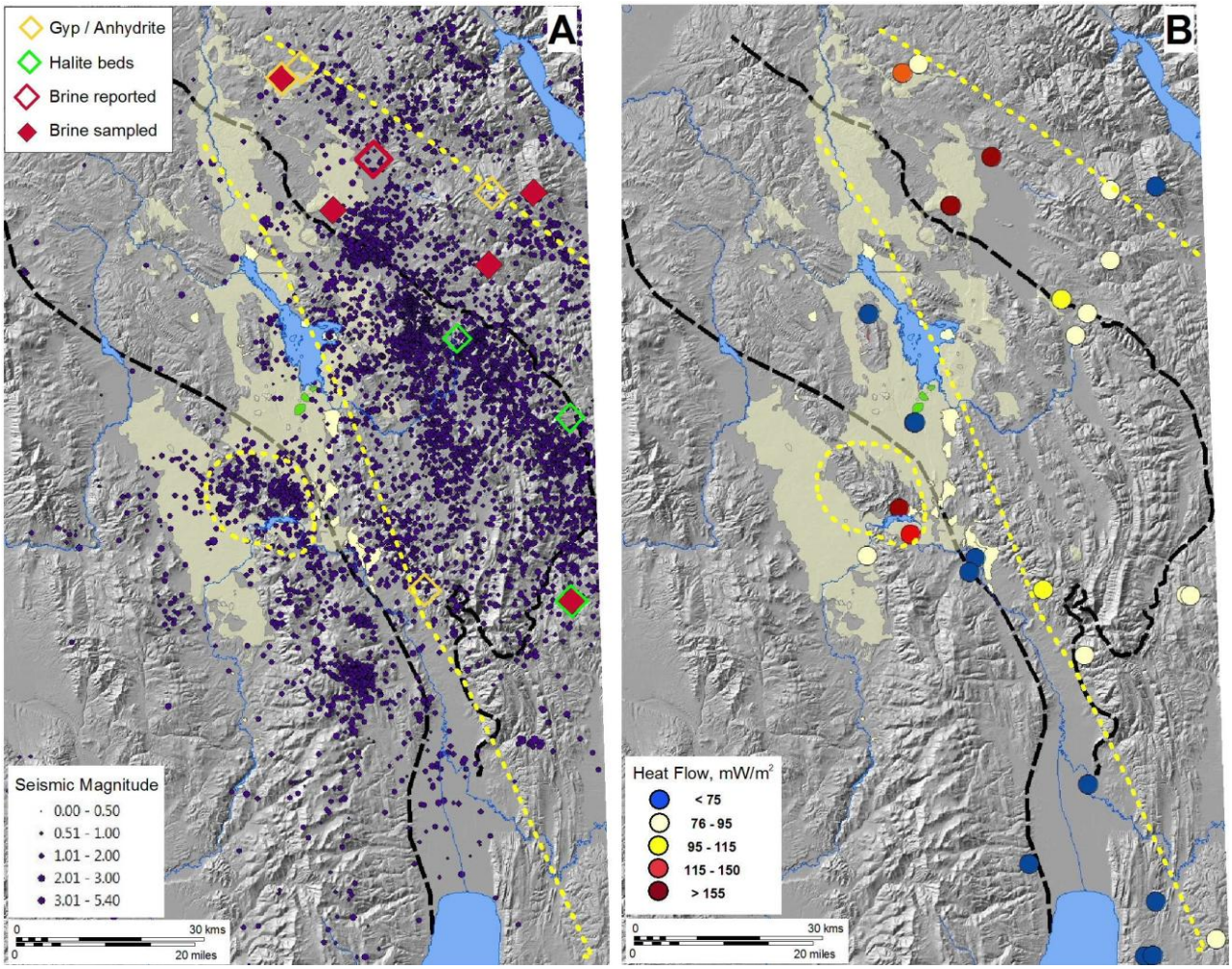

Figure 8 – Coincident patterns of (A) seismicity and (B) heat flow in the ITB. Areas of elevated heat flow are indicated by dashed yellow lines. Symbology in (A) indicates locations where saline fluid / brine, massive halite beds, and gypsum / anhydrite were encountered in the subsurface. The pattern of seismicity suggests the possibility that halite dissolution and roof collapse in the Preuss Sandstone may be occurring in response to hydrothermal fluid movement in the sedimentary section.

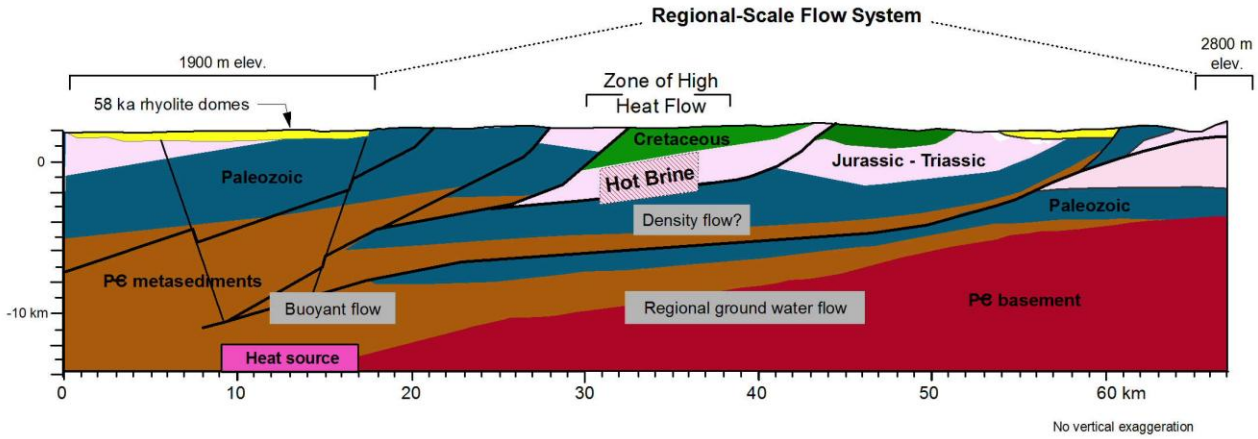

Figure 9 – Conceptual model of the BVF / ITB geothermal system based on Dixon's (1982) cross-section 9. Heat and mass transport conditions and thermal effects of the heat source, the impact of regional anisotropy, and the effects of density-driven flow vs. thermal buoyancy and their interaction with regional ground water flow will need to be evaluated.

4.2 Hypotheses and Questions

Advective Heat Transport – Advective transport appears to be necessary to explain the low heat flow observed within the China Hat graben and the high heat flow to the east. If so, then the magnitude of hydraulic anisotropy (K_H/K_V) required to initiate eastward buoyancy-driven flow into the rocks of the ITB will be a high priority for future modeling efforts. Thrust faults may impose large-scale anisotropy via internal permeability contrasts arising from brecciation and fault gouge along the faults (Ralston et al., 1983; Forster and Evans, 1991) or indirectly, by juxtaposing high- and low-permeability formations that can channel fluid flow sub-parallel to the thrust planes.

Impact of Dissolved Salt on Hydrothermal Circulation – Massive halite interbeds in the Preuss Sandstone, up to several hundred meters cumulative thickness, were encountered in three wildcat wells in the zone of high heat flow and appear to be the predominant source of salt in these hot brines. However, these saline fluids have been encountered as far down in the stratigraphic section as the Pennsylvanian Wells Formation. Whether other sources of halite exist lower in the section, or whether saline waters generated in the Preuss are redistributed vertically via density-driven flow, needs to be evaluated quantitatively. The sole lithium analysis available for these fluids (Table 2) suggests that the brines may be much richer in lithium than Salton Sea geothermal brines, possibly the result of mobilization from a Li-rich magma (Hofstra et al., 2013).

Seismic Swarms and the Role of Salt Dissolution – Demonstrating whether a relationship exists between high heat flow, salt dissolution, and microseismicity will be extremely important to understanding the spatial distribution of heat, hydrothermal circulation, and secondary porosity in this system. The seismicity is characterized by local swarms of small-magnitude events ($M<2$) at depths that may coincide with the Preuss salt beds. We plan to analyze selected swarms during 2007-2009, when high-resolution seismic data were captured, in order to identify focal mechanisms and hypocentral depths and to determine whether these events are of tectonic origin or if they reflect the collapse of cavernous salt porosity that has developed in the Preuss Sandstone.

Location of the Magmatic Heat Source – Can an arrangement of heat source, flow paths and reservoir rocks similar to the conceptual model in Figure 9 explain the advective transport of magmatic heat into the Mesozoic and Paleozoic rocks of the ITB, or might the heat source be located farther east of the China Hat graben, such that hydrothermal flow is vertically localized beneath the zone of high heat flow? Related to this question is the striking coincidence of potential hydrothermal indicators at the south end of the BVF, including high heat flow and localized seismicity (Figure 8), very high CO_2 flux (including magmatic helium) and elevated concentrations of volatile elements (F, As, Ba, S) in travertines (S.R. Ohly, in prep.), as well as the vapor-dominated geothermal activity in Sulfur Canyon at the southeast end of the BVF. Are all these observations a manifestation of magmatic outgassing along a separate flow path from those sustaining the heat flow anomaly to the east, or is this activity simply the least well-hidden manifestation of high-temperature hydrothermal processes in an otherwise very well-hidden geothermal system?

5. CONCLUSIONS

A synthesis of data compiled for the National Geothermal Data System, augmented with newly acquired shallow heat flow data, has revealed the existence of a previously unrecognized high-temperature magmatic hydrothermal system in the western ITB where it transitions into the B&R and where evidence points to significant ongoing magmatic outgassing from a robust heat source associated with the parent magma of China Hat's 58 ka rhyolites. Heat flow data collected from three new shallow gradient wells have clarified the pattern of low heat flow within the China Hat graben, and an analysis of thermal data from deep wildcat petroleum wells drilled in the ITB has defined a large area of high heat flow (100-200 mW/m^2) to the east of the graben. This zone is associated with high-temperature fluids (160-220 ^oC) in Jurassic to Pennsylvanian rocks at depths of 3-5 km, some of which may have good reservoir potential. According to the economic temperature-depth envelope defined by Allis et al. (2013) for hot sedimentary reservoirs, this resource could have economic potential if adequate porosity and permeability are available.

The chemical composition of these hot fluids is dominated by sodium and chloride with variable amounts of sulfate. However, the possible range of salinity is poorly constrained, with observed total dissolved solids ranging from less than 10 grams/liter to over 300 grams/liter, most likely because of dilution incurred during sampling in the DST. No information is available on the spatial or stratigraphic variability of either fluid density or chemistry that characterizes this resource. Although speculative at this stage, the one analysis of lithium content found in DST reports suggests that these brines could have economic potential as a lithium resource. A recent synthesis of data on lithium-rich "topaz" rhyolites and their spatial association with lithium-rich brines (Hofstra et al., 2013) suggests that China Hat's magma (also a topaz rhyolite) could be the source of the high lithium in the one brine sample.

The volcanic and geothermal setting of the BVF - ITB resource makes this a unique type of hot sedimentary geothermal prospect. However, the geochemical signatures and spatial relationships in thermal and non-thermal waters of the study area suggest the possibility that hot fluids of similar composition may not be restricted to the western ITB and may occur elsewhere in the thrust belt (Welhan, 2014). Thermal waters of similar Na-Cl composition are observed as far apart as Heise Hot Springs, 100 km north of China Hat, the East Bingham well near the Idaho-Utah border (inset, Figure 7), as well as Crystal Hot Springs and the Davis #1 geothermal exploration well, both near Brigham City, Utah (Austin et al., 2006). These fluids are compositionally similar and share similar stratigraphic and structural settings and may all reflect northern B&R crustal heat flow and/or magmatic influences.

REFERENCES

Allis, R., J.N. Moore, T. Anderson, M. Deo, S. Krby, R. Roehner and T. Spencer, 2013, Characterizing the power potential of hot stratigraphic reservoirs in the western U.S., Proc., Thirty-Eighth Workshop on Geothermal Reservoir Engineering, Stanford Univ., SGP-TR-198.

Armstrong, F.C., 1969, Geologic map of the Soda Springs Quadrangle, southeastern Idaho, Misc. Geol. Investigations Map I-557.

Armstrong, F.C. and S.S. Oriel, 1965, Tectonic development of the Idaho-Wyoming thrust belt, Bull. Am. Assoc. Petroleum Geologists, **49**, 1847-1866.

Austin, C.F., R. Austin and M.C. Erskine, 2006, Renaissance a geothermal resource in northern Utah, GRC Trans., **30**, 853-858.

Autenrieth, K.D., M. McCurry, J. Welhan and S. Polun, 2011, Conceptual subsurface model of the Blackfoot volcanic field, southeast Idaho: A potential hidden geothermal resources, GRC Trans., **35**, 695-697.

Avery, C., 1987, Chemistry of thermal water and estimated reservoir temperatures in southeastern Idaho, north-central Utah and southwestern Wyoming, Wyoming Geol. Survey 38th Field Conf., 347-353.

Blackwell, D.D., 1983, Heat flow in the northern Basin and Range province; in The Role of Heat in the Development of Energy and Mineral Resources in the Northern Basin and Range Province, GRC Special Report **13**, 81-93.

Blackwell, D.D., 1989, Regional implications of heat flow of the Snake River Plain, Northwestern United States, Tectonophysics **164**, 323-343.

Blackwell, D.D., and M. Richards, 2004, Calibration of the AAPG geothermal survey of North America BHT database, AAPG Meeting, Dallas, Texas, April 2004, Southern Methodist Univ. Geothermal Lab poster on BHT calibration, URL: http://smu.edu/geothermal/BHT/BHT.htm

Bones, D. G., 1978, Seismicity of the Intermountain Seismic Belt in southeastern Idaho and western Wyoming, and tectonic implications, Univ. of Utah M.S. thesis, 260 pp.

Brott, D., D. Blackwell and J. C. Mitchell, 1976, Heat flow study of the Snake River Plain, Idaho, Geothermal Investigations in Idaho, Part 8, Water Information Bull. 30, Idaho Dept. Water Resources.

Buck, B.W. and B. Winegar, 2003, Integration of surface water management with mitigation of ground water impacts at a proposed phosphate mine overburden facility; Joint Conference - Billings Land Reclamation Symposium and American Society of Mining and Reclamation, June 3-6, Billings, Montana, http://www.jbrenv.com/news/view/11

Clarke, E.C.W. and D.N. Glew, 1985, Evaluation of the thermodynamic functions for aqueous sodium chloride from equilibrium and calorimetric measurements below 154 ^{o}C; J. Phys. Chem. Ref. Data, **14**, 489-610.

Dion, N.P., 1974, An estimate of leakage from Blackfoot Reservoir to Bear River Basin, southeastern Idaho, Idaho Dept. Water Admin., Water Information Bull. **34**, 24 pp.

Dixon, J.S., 1982, Regional structural synthesis, Wyoming Salient of western overthrust belt. Bull. Am. Assoc. Petroleum Geologists, **66**, 1560-1580.

Edwards, M.C., 2013, Geothermal resource assessment of the Basin and Range Province in western Utah, Univ. of Utah M.S. thesis, 113 pp.

EERE, 2011, Technologies for extracting valuable metals and compounds from geothermal fluids; U.S. Dept. of Energy, http://www4.eere.energy.gov/geothermal/projects/169

Ford, M.F., 2005, The petrogenesis of Quaternary rhyolite domes in the bimodal Blackfoot volcanic field, southeastern Idaho, Idaho State Univ. M.S. thesis, 133 pp.

Forster, C.B. and J.P. Evans, 1991, Hydrogeology of thrust faults and crystalline thrust sheets: Results of Combined Field and Modeling Studies; Geophys. Research Letters, **18**, 979-982.

Harbour, J.L. and R.M. Breckenridge, 1980, Summary of the overthrust belt in parts of Wyoming, Utah, and Idaho; Idaho Geological Survey Tech. Report **80-9**, 6 pp.

Harrison, W.E., K.V. Luza, M.L Prater, and P.K. Chueng, 1983, Geothermal resource assessment of Oklahoma, Special Publication **83-1**, Oklahoma Geol. Survey,42 pp.

Henrikson, A., 2000, New heat flow determinations from oil and gas wells in the Colorado Plateau and Basin and Range of Utah, Univ. of Utah M.S. thesis, 69 pp.

Henrikson, A. and D.S. Chapman, 2002, Terrestrial heat flow in Utah; unpubl. report, Univ. of Utah; http://geology.utah.gov/emp/geothermal/pdf/terrestrialhf.pdf

Heumann, A, 1999, Timescales of processes within silicic magma chambers. Netherlands Research School of Sedimentary Geology (NSF) Publication No. 991001, PhD Dissertation, 197 pp.

Hofstra, A.H., T.I. Todorov, C.N. Mercer, D.T. Adams and E.E. Marsh, 2013, Silicate melt inclusion evidence for extreme pre-eruptive enrichment and post-eruptive depletion of lithium in silicic volcanic rocks of the western United States: Implications for the origin of lithium-rich brines, Economic Geology, **108**, 1691-1701.

Hutsinpiller, A. and W.T. Parry, 1985, Geochemistry and geothermometry of spring waters from the Blackfoot Reservoir region, southeastem Idaho; J. Volcanology Geothermal Research, **26**, 275-296.

IDWR, 1980, Geothermal resources of Idaho; Part 9, Water Information Bull. No. 30, Idaho Dept. of Water Resources, Plate 1, 1:500,000 scale map.

IGS, 2013, Idaho Oil and Gas Wells, 1903-1988; http://www.idahogeology.org/services/Oilandgas/

Lachenbruch, A.H., J.H. Sass and P. Morgan, 1994, Thermal regime of the southern Basin and Range province; Implications of heat flow for regional extension and metamorphic core complexes, J. Geophysical Research, **99**, 22121-22133.

Lewicki, J.L., G.E. Hilley, L. Dobeck, T.L. McLing, B.M. Kennedy, M. Bill and B.D.V. Marino, 2012, Geologic CO2 input into groundwater and the atmosphere, Soda Springs, ID, Chem. Geology, **339**, 61-70.

McCurry, M. and J.A. Welhan, 2012, Do magmatic-related geothermal energy resources exist in southeast Idaho? GRC Trans., **36**, 699-707.

Mitchell, J.C., 1976, Geochemistry and geologic setting of the thermal and mineral waters of the Blackfoot Reservoir Area, Caribou County, ldaho; Geothermal Investigations in Idaho, Part 6, Water Information Bull. 30, Idaho Dept. Water Resources, 47 pp.

Mitchell, J.C., L.L. Johnson and J.E. Anderson, 1980, Plate 1, Potential for direct heat application of geothermal resources; Geothermal Investigations in Idaho, Part 9, Water Information Bull. 30, Idaho Dept. Water Resources, 396 pp.

Morgan, P., and B. Scott, 2011, Bottom-hole temperature data from the Piceance Basin, Colorado: Indications for prospective sedimentary basin EGS resources, GRC Trans., **35**, 477-485.

Mulvaney, L. and J. Kaskey, 2012, Lithium boom spurs production from brine, Bloomberg News http://www.bloomberg.com/news/2012-09-19/lithium-boom-spurs-production-from-california-brine-commodities.html

NGDS, 2012, Idaho-specific geothermal data; AASG Geothermal Data Repository, National Geothermal Data Sytem, http://repository.stategeothermaldata.org/repository/browse/

Ott, V.D., 1979, Geology of the Woodruff Narrows Quadrangle, Utah-Wyoming, Brigham Young Univ. M.S. thesis.

Ott, V.D., 1980, Geology of the Woodruff Narrows Quadrangle, Utah-Wyoming; in Brigham Young Univ. Geology Studies, W.K. Hamblin and C.M. Gardner (eds.), pp. 67-84.

Pickett, K.E., 2004, Physical volcanology, petrography, and geochemistry of basalts in the bimodal Blackfoot volcanic field, southeastern Idaho, M.S. thesis, Idaho State Univ., 92 pp.

Pollack, H.N., S.J. Hurter and J.R. Johnson, 1993, Heat flow from the earth's interior: Analysis of the global data set, Rev. Geophysics, **31**, 2667-280.

Polun, S.G., 2011, Kinematic analysis of Late Pleistocene faulting in the Blackfoot lava field, Caribou County, Idaho, Idaho State Univ. M.S. Thesis, 86 pp.

Polun, S.G., D.W. Rodgers and M. McCurry, 2010, New kinematic analysis of late Pleistocene faulting in the Blackfoot rift zone, Idaho, USA; Geol. Soc. America, Abstracts with Programs, **43**, 54.

Ralston, D.R. and R.E. Williams, 1979, Groundwater flow systems in the western phosphate field in Idaho, J. Hydrology, **43**, 239-264.

Ralston, D.R., J.L. Arrigo, J.V. Baglio, L.M. Coleman, J.M. Hubbell, K. Souder and A.L. Mayo, 1983, Thermal ground water flow systems in the thrust zone of southeastern Idaho, U.S. Dept. of Energy DOE/ET/ 28407-4 (DE84011598), 336 pp.

Reed, M. and N. Spycher, 1984, Calculation of pH and mineral equilibria in hydrothermal waters with application to geothermometry and studies of boiling and dilution; Geochim. Cosmochim. Acta, **48**, 1479-1492.

Schmitt, A.K., 2011, Uranium-series accessory crystal dating of magmatic processes; Annual Rev. Earth Planet. Sci., **39**, 321-349.

Simplot, 2005, Site Investigation Report Smoky Canyon Mine, Caribou County, Idaho; report prepared for J.R. Simplot Company by NewFields, LLC, 43 pp. plus addendices.

Simplot, 2010, Conda/Woodall Mountain Mine Pedro Creek overburden disposal area early action: Engineering evaluation/cost analysis; report prepared for J.R. Simplot Company by Formation Environmental, LLC, 121 pp. plus appendices.

Smith, R.L. and H.R. Shaw, 1979, Igneous-related geothermal systems; in L.J.P. Muffler (ed.) Assessment of Geothermal Resources of the United States—1978; U.S. Geol. Survey Circ. **790**, 10-17.

Smith, R.L., H.R. Shaw, R.G. Luedke and S.L. Russell, 1978, Comprehensive tables giving physical data and thermal energy estimates for young igneous systems of the United States; U.S. Geol. Survey Open-File Report **78-925**, 28 pp.

SMU, 2008, Southern Methodist Univ. Geothermal Laboratory heat flow database; http://smu.edu/geothermal

USArray, (2013), Incorporated Research Institutions for Seismology, http://www.usarray.org/

USFS, 2011, South Maybe Canyon Mine site engineering evaluation/cost analysis for an interim removal action for the Cross Valley fill; report prepared for U.S. Forest Service by Millenium Science & Engineering, Inc., 99 pp. plus appendices.

Welhan, J.A.. 2014, The Blackfoot volcanic field and Idaho thrust belt geothermal prospect: Final report and data summary, National Geothermal Data System final project report (in prep.).

Welhan, J.A., D. Garwood, and D. Feeney, 2013, The Blackfoot volcanic field, southeast Idaho: A hidden high-T geothermal resource revealed through data mining of the National Geothermal Data Repository, GRC Trans., **37**, 365-374.

White D.E., Muffler, L.J.P. and Truesdell, A.H., 1971, Vapor-dominated hydrothermal systems compared with hot-water systems, Economic Geology, **66**, 75-97.

Whyatt, J. and F. Varley, 2013, Catastrophic failures of underground evaporate mines, http://www.cdc.gov/niosh/mining/Userfiles/works/pdfs/cfoue.pdf

WRCC, 2013, Western Regional Climate Center, wrcc@dri.edu